

Light Reallocation for High Contrast Projection Using an Analog Micromirror Array

Reynald Hoskinson*

Boris Stoeber

Wolfgang Heidrich

Sidney Fels

The University of British Columbia



Figure 1: Left: our prototype projector that uses an analog micromirror array to re-allocate light from dark to bright image regions, thus achieving higher contrast and peak brightness than normal projector designs. Center and Right: two photographs of the same projected image taken at different exposures. Details in one image that are not visible in the other reveal the added contrast due to our projector design.

Abstract

We demonstrate for the first time a proof of concept projector with a secondary array of individually controllable, analog micromirrors added to improve the contrast and peak brightness of conventional projectors. The micromirrors reallocate the light of the projector lamp from the dark parts towards the light parts of the image, before it reaches the primary image modulator. Each element of the analog micromirror array can be tipped/tilted to divert portions of the light from the lamp in two dimensions. By directing these mirrors on an image-dependent basis, we can increase both the peak intensity of the projected image as well as its contrast.

In this paper, we describe and analyze the optical design for projectors using this light reallocation approach. We also discuss software algorithms to compute the best light reallocation pattern for a given input image, using the constraints of real hardware. We perform extensive simulations of this process to evaluate image quality and performance characteristics of this process. Finally, we present a first proof-of-concept implementation of this approach using a prototype analog micromirror device.

CR Categories:

B.4.2 [INPUT/OUTPUT AND DATA COMMUNICATIONS]: Input/Output Devices—Image display; I.3.3 [COMPUTER GRAPHICS]: Picture/Image generation—Display algorithms I.4.0 [IMAGE PROCESSING AND COMPUTER VISION]: General—Image displays

Keywords: high dynamic range, projection, contrast

*e-mail: reynald@ece.ubc.ca, stoeber@mech.ubc.ca, heidrich@cs.ubc.ca, ssfels@ece.ubc.ca

1 Introduction

Video projectors are carefully engineered to maximize the percentage of the light from the lamp that reaches the spatial light modulator (SLM), and to relay the formed image through the projection optics onto the screen with the lowest loss of light possible. The SLM is evaluated by how well it passes light, and also how well it blocks it, because it is its ability to block light that ultimately creates the image seen on the screen. The SLM in a projector is usually a liquid crystal display (LCD) or a digital micromirror device (DMD) that selectively reduces the illumination of pixels on the screen in order to form the dark parts of the image. For instance, a DMD is an array of micromirrors, one for each pixel, each one of which can be tilted in one direction so that incident light reflects towards the projection lens and then out onto the screen, or another direction so the light is reflected to a heat sink and that spot on the screen remains dark. How efficient the projector is at doing this has major repercussions. Brightness is the primary characteristic determining projector price and quality, and projector efficiency is one key in determining the final brightness of the projected image. Moreover, currently available SLMs “leak”, that is, they do not block all the light for black image areas, thus limiting contrast [Dewald et al. 2004].

To increase the brightness of the projected image, simply increasing the brightness of the lamp is not always a realistic option. The lamp is typically the most expensive piece of the projector, even more so than the SLM. Since the light that is not directed to the screen ends up as heat, a brighter lamp carries with it the need for bulkier and noisier fans and lamp electronics. No matter how carefully the lamp reflector and relay optics are engineered, a fundamental limitation on efficiency is encountered: the image is formed by letting light through to the screen for the bright parts of the image, and blocking the light for the dark regions. The light source in a projector supplies a uniform brightness distribution on the primary spatial light modulator, limiting the maximum brightness for a displayed image. For most images, however, only a fraction of the total area is illuminated at peak brightness, so much of the light is lost no matter how efficient the modulator.

To address the contrast shortcomings of currently available pro-

jectors, we have built a proof-of-concept projector with a low-resolution secondary mirror array that in effect turns the single lamp inside a projector into a multitude of light sources that can each be moved to where they are needed in the image. The secondary mirror device is capable of directing the uniform light from the projector lamp incident on its surface to different areas on the light modulator, in effect projecting a low-resolution version of the original image onto the light modulator.

Adding this analog mirror device improves the dynamic range in two ways: by directing the light to the bright parts of the image, the achievable peak brightness will be increased. Simultaneously, the amount of light that needs to be blocked in the dark regions of the image will be reduced, thus decreasing the brightness of the black level. This light redirection is realized with a low-resolution analog micromirror array (AMA), fabricated using microelectromechanical system (MEMS) technology. The tip and tilt angle (two degrees of freedom) of the micromirrors in the array can be set continuously in order to direct light to an arbitrary location on the light modulator.

A projector using our design would be particularly suited to displaying high-dynamic range (HDR) images in an efficient manner. The AMA device closely parallels the use of a second, low-resolution spatial light modulator in HDR displays [Seetzen et al. 2004]. Unlike earlier approaches for HDR projection (e.g. [Damberg et al. 2007; Pavlovych and Stuerzlinger 2005]), our design reallocates rather than absorbs unwanted light. We are therefore able to improve energy efficiency and reduce heat generation in much the same way as Seetzen et al.’s [2004] LED display design improves efficiency over their initial double-absorption design.

However, there are also significant differences between our light reallocation approach and the original dual-modulation HDR displays. The most important difference is that the total amount of light can be varied in Seetzen et al.’s work, while it is fixed in our case. Furthermore, the physical constraints of AMA devices result in a limited maximum spatial displacement of light, which imposes additional constraints on the light allocation. These differences mandate new algorithms for light allocation, which we present in this paper, along with the physical and optical design principles of light reallocation projectors.

2 Related work

The concept of using a secondary mirror array was originally suggested in [Hoskinson and Stoeber 2008], but no proof-of-concept was developed, and there was no detailed optical analysis. This work offers the first physical evidence of such an arrangement, and presents a more efficient allocation algorithm for making use of the light from the secondary mirror array.

The AMA acts as a second, low-resolution modulator, similar to the system described by Seetzen et al. [2004], where a low-resolution individually-controllable array of LEDs behind a high-resolution LCD screen functions as a second modulator. The light distribution of the low-resolution modulator is then corrected by the high-resolution modulator to achieve the desired image. In the work by Seetzen et al., the LEDs are in fixed locations, irrespective of where the bright parts of the image are. In our approach, the backlight is instead composed of an array of spots of constant intensity, and each spot can be moved across the image plane. This means that light can be targeted to exactly where it is needed, for example boosting the peak brightness by directing multiple light spots into the same spatial location.

The concept of using two light modulators in series put forward by Seetzen et al. [2004] has primarily been applied to flat-panel

displays, but has also been applied to several projector designs. Conventional projectors use high-intensity discharge (HID) lamps, which are not suitable for placement in a tightly-packed array, and typically operate efficiently only at one output intensity, so HID lamps are not themselves suitable as modulators. Instead, some approaches (e.g. [Pavlovych and Stuerzlinger 2005; Damberg et al. 2007; Kusakabe et al. 2009]) improve projector contrast by adding a second LCD modulator into the light path, which significantly reduces the overall black level of the system, but at the cost of a significant reduction in overall brightness, as black and white LCD panels typically transmit only 30-35% of unpolarized incident light. Matching polarization between the two LCD modulators so that only one polarization step is required only reduces the amount of loss, it does not eliminate it.

A more fundamental problem is that additional absorption only adds extra bits of information at the dark end of the intensity range. This additional dynamic range is in practice only useful in dark rooms, since ambient illumination otherwise dominates that intensity range. Although we are not aware of any systems that employ two DMDs in series, they would also improve solely in the dark intensities. Increasing useful dynamic range with these projector designs therefore requires brighter HID lights at significantly increased expense, power consumption, and heat production. Our design, on the other hand, can increase peak intensity without a change in light source.

Both Bimber [2008] and Seetzen [2009] have suggested other approaches to HDR projection that involve superimposing a projected image onto a paper print or a reflective display, such as e-ink. The advantage of this approach is that the change in reflectance affects both the light arriving from the projector, as well as the reflected ambient illumination, which makes this approach useful even in illuminated rooms. However, Bimber’s approach is designed only for static images such as X-rays. While Seetzen’s approach takes advantage of interactive reflective displays such as e-ink to display dynamic images, current e-ink displays are still too slow for practical implementations of this concept, and screens of suitable size would likely be prohibitively expensive. Seetzen’s also proposes the use of an array of hundreds or thousands of very small projectors with individual modulated light sources such as LEDs. This proposal has not yet been implemented in full scale, but one would expect the calibration and alignment issues to be severe.

Some recent commercial projectors include a dynamic iris, a physical aperture near the lamp that can change size with each video frame, thus limiting the total illumination that reaches the screen [Iisaka et al. 2003; Toyooka et al. 2005]. While this method can decrease the black level of certain images, this is only a global adjustment that does not allow for contrast improvements within a single image. In addition, our approach could easily be combined with a dynamic iris to produce even higher temporal dynamic range.

Lasers have also been used as a light source for projectors, in the following three forms:

1. As a raster scanner, with a laser for each primary color, combined to one spot showing one pixel at a time. The spot moves over the image quickly enough so that each image is integrated by a human observer. The laser intensity is modulated at video rate.
2. Linear arrays such as the grating light valve [1997], which produce the image through diffractive elements, one line at a time. A scanning mirror moves the single line through the image over time.
3. As a conventional light source, with a DMD or other light valve technology.

The primary reason the lasers have so far been kept out of commodity displays is cost per lumen: laser sources bright enough for most forms of commodity projectors continue to be commercially cost-prohibitive.

Conceivably, the time that a scanning laser spends at each pixel could be varied to achieve a similar result as in this paper. The problem is that all raster-scanning laser projectors we are aware of use single or dual scanning mirrors tilting at resonance. This is mechanically very advantageous, but also prevents varying laser/pixel exposure time. Doing so would involve a complete redesign of all mechanics. Laser projectors using linear arrays make use of diffraction, and thus would be unsuitable for this sort of change. Using lasers as conventional light sources, on the other hand, would be compatible with our system.

3 Optical system design

3.1 Spot position, size on spatial light valve

Our prototype is limited by the hardware available to us on an academic budget, including analog micromirrors with less-than-ideal functionality which constrain our results to a basic proof of concept. We therefore devote a considerable portion of this work to theoretically quantifying the limits and opportunities of the AMA approach.

Figure 2 shows the traversal of one bundle of rays through a projector following our design. The AMA would work with any type of spatial light modulator; here we illustrate with a single-chip digital-light projection (DLP) projector. First in the light path, a reflector collects the light from a small arc lamp, and directs it to the illumination optics. The lamp reflector minimizes the spot size of the light at the color wheel. Next is the integrator, which spatially redistributes the image of the arc from a highly-peaked to a more uniform distribution with an aspect ratio that matches that of the light modulator. In our design, the light is then reflected off of an AMA device, which spatially redirects light to different parts of the light modulator, in this case a DMD. The image of the DMD is finally transmitted to the screen using a projection lens system. For best utility, the spot size of light from each AMA element should be minimized when it reaches the DMD, while the spot displacement for a given mirror tilt angle should be maximized.

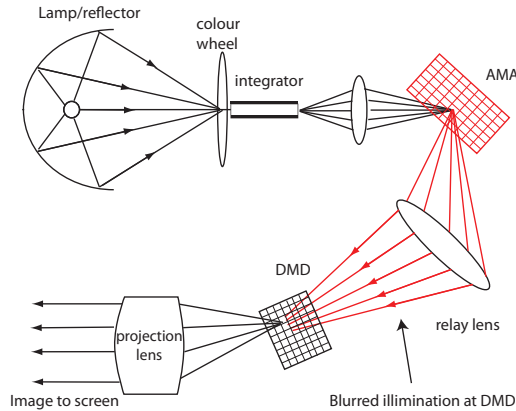


Figure 2: Light path of projector with an AMA, showing one ray bundle.

The optical path from the AMA to the DMD is shown schemat-

ically in Figure 3. The simple thin lens formula [Hecht 2002] $1/f = 1/u + 1/v$ gives a relationship between the distance from object to lens u , distance of image to lens v , and lens focal length f . As shown by the dashed lines in Figure 3a, a point on the object plane u is mapped to an in-focus spot on the image plane v . If the AMA was placed at u , the spot size of the AMA mirror would be minimized. However, in that configuration, every point on the object plane would be mapped to a corresponding point on the image plane. Tilting the mirrors would therefore not move the light from one region to another when the AMA is in focus on the DMD. If anything, the light from a tilted mirror of the AMA would be blocked by the aperture of this relay lens and not make it to the DMD at all.

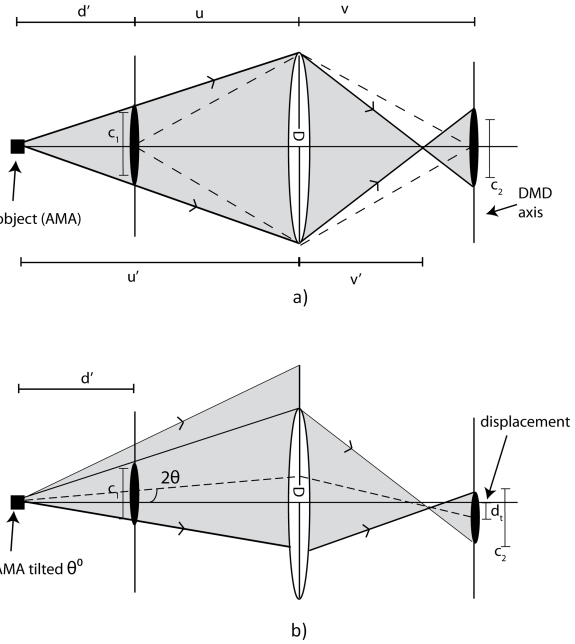


Figure 3: Illustration of circle of confusion. A point on the AMA spreads to a region c_1 , that in turn is imaged onto the DMD as the circle c_2 . In b), the mirror is tilted by θ , causing the light cone to be shifted by 2θ . The dotted line in b) represents the shifted principle ray of the cone.

To achieve the desired effect of redirecting light from one region to another, the AMA is placed at a distance d' from the object plane of the lens, as shown in Figure 3a. By the time the light from a point on the AMA reaches a distance u from the lens, it describes a circle c_1 , which in turn is imaged onto the DMD plane, forming the circle of confusion c_2 . This has the effect of blurring the image of the AMA at the DMD plane. Using simple geometry, we can see that c_1 is proportional to the lens (aperture) diameter D and the separation between AMA and focal plane, and that it is independent of the lens focal length. It can be calculated as

$$c_1 = \frac{D}{u'} |(u - u')| = \frac{D}{u'} d'. \quad (1)$$

The diameter c_2 of the circle of confusion on the image side of the lens is then $c_2 = |m|c_1$, where m is the magnification of the lens system, obtained by $m = -v/u$.

The final calculation for the diameter of the circle of confusion becomes

$$c_2 = |Dm \frac{d'}{u'}|. \quad (2)$$

The aperture D also limits the angular distribution of incoming light from the AMA. To lower the rate of increase of blur diameter as the disparity increases, we could reduce the aperture of the lens, but that would negatively affect the system efficiency of the projector. D should be of a size that makes its numerical aperture nearly equal to that of the DMD.

When an AMA mirror is tilted as shown in Figure 3b, the incident light is redirected for a distance d' before it reaches the object plane. Mirror motion therefore leads to a spatial displacement of a spot-shaped portion of light. We call these *light spots* (light spot). The displacement d_t at the DMD plane is

$$d_t = md' \tan(2\theta). \quad (3)$$

From Equations 1 and 3 it is evident that as we increase the separation d' to increase the displacement of the light spot on the DMD, the circle of confusion also grows, so we are blurring the light from the AMA mirror. The magnification affects both the displacement and the blur. Increasing the magnification m of the AMA on the DMD would increase d' , but would also increase the blur c_2 by the same factor. Likewise, if the AMA was much bigger than the DMD, $m < 1$ would decrease the blur, but also decrease d' , and thus reduce the range of the light spot on the DMD. Magnification is therefore not a useful way of manipulating blur.

3.2 Luminance clipping due to AMA tilt

At its most fundamental level, reallocating the light using an AMA involves fitting the intensity distribution from the lamp as closely as possible to that of the image, while staying within the limits imposed by the **étendue** of the projector. Étendue is the geometric capability of an optical system to transmit light [Brennesholtz and Stupp 2008], and can be defined as

$$E = \int \int \cos \theta dA d\Omega, \quad (4)$$

where E is integrated over the area of interest. The angle θ is between the centroid of the solid angle element $d\Omega$ and the normal to the surface element dA . Note that there is no term in this equation relating to optical intensity: étendue is solely a geometric property. When a beam is modified by a well-corrected optical element, étendue is preserved. For example, when a lens focuses a beam to a spot, the area of the beam is reduced but the convergence angle of the beam increases, so étendue is preserved. The étendue of a ray bundle of light can never decrease; in an area that involves scattering, it will increase. In a projector, the SLM is usually the element with the smallest étendue.

When the AMA mirrors tilt, they change the location of the light at the DMD as desired, but also affect its local angular distribution and thus the étendue of the beam. As a result, some of the redistributed light will be clipped by the pupil of the projection lens. To quantify the clipping, we determine the effect that a tilted AMA mirror has on a ray as it travels to the DMD. As a first approximation, we trace an affected ray's path through a single thin-lens system using the matrix method described by Halbach [1964]. With this formulation, the angular difference α' resulting from diverting the initial ray by α using the AMA is $\alpha - (\alpha u')/f$, where u' is defined

in Figure 3. We can use the Newtonian expression for magnification [Hecht 2002] $m = -f/x_o$, where $x_o = u' - f$ to arrive at the expression for the change in angle of a diverted ray as

$$\alpha' = \frac{\alpha}{m}. \quad (5)$$

Equation 5 shows that, if we begin with a large AMA so that the magnification onto the DMD is less than 1, the angular change at the DMD is increased, leading to more clipping at the DMD aperture. A large magnification, on the other hand, adversely affects the circle of confusion as calculated in Equation 2. The desired tilt angle of the AMA therefore becomes a compromise between the flexibility of large displacements and the necessity to limit clipping.

To some degree, clipping is mitigated by the non-uniform angular distribution of the light source in a projector. We take this into account using the weighting of light intensity as a function of angle for a projection lamp given in [Derra et al. 2005]. Figure 4 shows the resulting losses as a function of the mechanical tilt angle of the AMA mirror, for a UHP lamp with a 1mm arc length, and a DMD with 12° tilt angle and an area of $14.1\text{mm} \times 10.5\text{mm}$. It shows that the tilt angle of the AMA should be minimized to reduce extra system losses. At a 2.5° tilt angle, the expected loss from clipping is 10%.

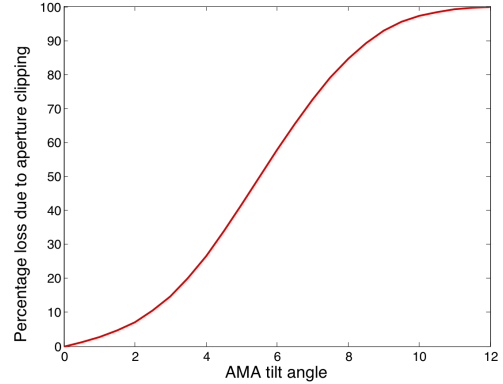


Figure 4: Estimated losses for AMA tilts due to the DMD aperture.

The distribution of light energy within the circle of confusion is given by the point-spread function (PSF). An approximation for the PSF that mimics the effect of system aberrations is given by Nagahara et al. [2008]:

$$p(r, c) = \frac{2}{\pi(gc)^2} e^{\frac{-2r^2}{(gc)^2}}, \quad (6)$$

where g is a constant that can be determined through an optical simulation for a given light source, or empirically through optical measurements, c is the diameter of the circle of confusion, and r is the distance of the image point from the center of the blur circle. The distribution of light from one whole light spot as it reaches the DMD, can be estimated by convolving the area of the mirror with the PSF. To obtain the final light distribution from the AMA, we calculate the displacement and magnification of each AMA mirror, place each mirror's displaced and magnified spot into an image, and then convolve the entire image by the PSF. If the DMD and AMA are parallel, as in Figure 3, and disregarding any local lens aberrations or apodization of the light incident to the AMA, all light spots

will have equal shape. If the two chips are not parallel, the distribution of each light spot will need to be calculated separately, because each will have a different PSF, due to the differing distances between points on the AMA and points on the DMD.

4 Light allocation

Finding the optimal light distribution for the AMA corresponds to choosing the locations for each of the n light spots from the array of n analog micromirrors. It is assumed that there is adequate granularity in the mirror control to position a light spot at any pixel in the image. To guide the allocation algorithm, we define an image improvement factor as the ability to boost the entire range of pixel brightness values, both dark and bright. This improvement is defined as a ratio, compared to a conventional projector design using the same DMD and light source without an AMA device. Since the AMA is only re-allocating rather than generating new light, this improvement factor is image-dependent. A uniform white image will see no improvement in peak brightness, while images with a few bright features on a dark background can be improved the most.

4.1 Gaussian pyramids

In [Hoskinson and Stoeber 2008], an approach using a Gaussian pyramid is described. Both the image and the light spot are low-pass filtered a number of times, each of which becomes a level of the pyramid. Starting at the coarsest level of the pyramid, the position of each of the light spots is iteratively adjusted towards the higher intensity regions, one at a time. This process is repeated down the pyramid to the finest level of detail.

4.2 Median cut approach

An alternative to allocating light spot via the process of analyzing a Gaussian pyramid is to divide the original image into equal energy zones, and allocate one light spot for each zone. The median cut algorithm described by Debevec [2005], a variation from the original described in Heckbert [1982], is an efficient method of subdividing an image into zones of approximately equal energy. Figure 5 shows an image cut into 28 regions. A light spot is placed with its center at the centroid of each region, here marked with squares. Using this approach, the image can be divided quickly into as many regions as there are light spots. With the Gaussian pyramid scheme, there are still many more pixels than there are spots at the coarsest level of the pyramid, so the initial allocation is much less representative of the actual intensity distribution of the pixels.

A light spot can have a limited range of movement from its original position due to the limited tilt angle of the micromirrors, which is not taken into account in the median cut algorithm. In the Euclidean bipartite minimum matching problem [Agarwal and Varadarajan 2004], we are given an equal number of points from two sets, and would like to match a point from one set with a distinct point from the other set, so that the sum of distances between the paired points is minimized. We can use an algorithm that solves this problem to match each centroid from the median cut step to a location of a light spot in its rest (non-tilted) state, and thus minimize the sum total distance between the pairs in the two groups. This will minimize the sum total angle that the mirrors must tilt to achieve the points specified in the median cut solution set.

The Euclidean bipartite matching problem can be solved in polynomial time using Kuhn’s Hungarian approach [1955]. The Hungarian approach does not support constraints such as maximum values for pairs, meaning that there might be some pairs that exceed the range of motion of an light spot for a given maximum mirror tilt

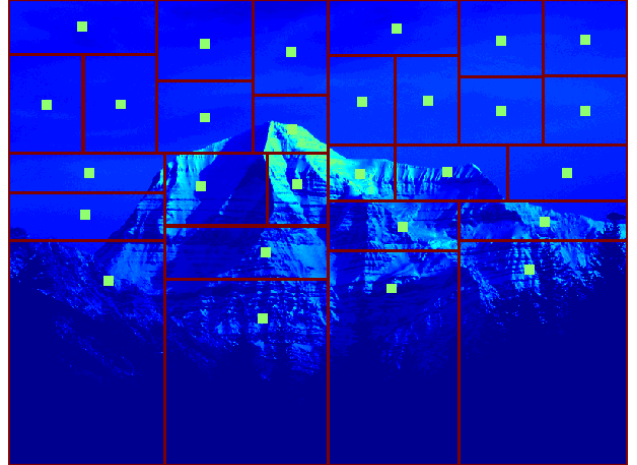


Figure 5: An image divided into 28 regions of roughly equal energy using the median cut algorithm. A light spot is placed at the centroid of each region (represented as dots).

angle. If any of the distances between the non-tilted light spot and the centroid are larger than the range, they are placed at the furthest point along the line that connects the two points. Figure 6 shows the results of using the median cut algorithm on the image in Figure 5.

In the end, the placement of each light spot provides a heterogeneous illumination I_p for the second modulator, in this case the DMD. We must correct for this variable illumination in the image that we send to the high-resolution modulator. The final result for the projected image will be a per-pixel optical multiplication of the two modulators: $kI_m(i, j) = I_{\text{DMD}}(i, j)I_p(i, j)$, where k represents the improvement in brightness. I_{DMD} is thus simply equal to $kI_m(i, j)/I_p(i, j)$, quantized to the 256 possible greyscale states of the DMD. The largest possible improvement factor k will depend on the luminance distribution of the image. If every single displayed pixel is required to have sufficient luminance, $k = \arg \min(I_p/I_m)$. At a higher k , some pixels cannot be reproduced at the luminance specified by kI_m .

4.3 Iterative adjustment

The solution obtained by using the median cut algorithm can be optimized by performing an iterative adjustment step. After the initial median cut solution is determined, the pixel with the minimum improvement is found, the closest light spot moved towards it, and the image improvement is evaluated at points along the path. The light spot is moved to the point along the path that scores highest. This process is repeated for each of the light spots until no movement towards the minimum improved pixel by any of the light spots results in a positive change.

5 Simulation results and analysis

The final achievable improvement k can be used to evaluate the choices for light spot size, range and number given as initial conditions to the simulation. The key variables are:

- **Range:** The distance, in pixels, along which a light source can move. This depends on the optical system and the maximum tilt angle achievable by the AMA micromirrors.
- **Blur:** The higher the disparity, the larger the blur, and also the larger the range of the mobile light source.

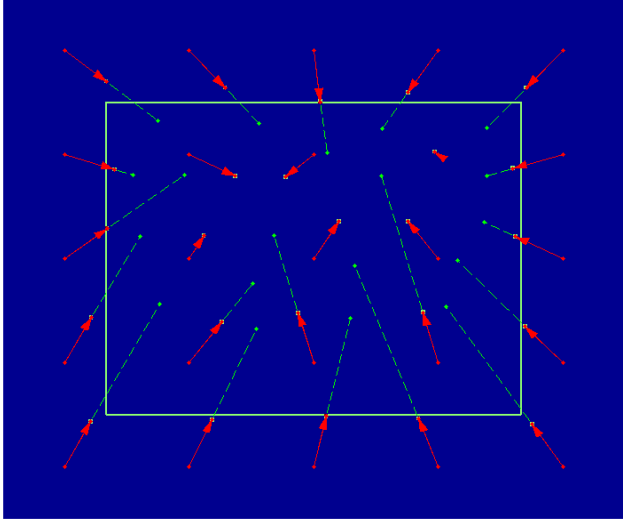


Figure 6: Diagram of placements of light spot for the image in Figure 5 using the median cut algorithm, with a mirror range of 100 pixels. The starting (small red dots) and ending (arrowheads) locations of each light spot are shown, as well as where they would have gone had they had unlimited range (green dotted line). The border of the SLM is shown as a rectangle. Some of the light spot start from beyond the border because of the required overfill to achieve a uniform illumination of the SLM.

- **Number of mirrors:** The number of mirrors within the AMA. With more mirrors, more details in the image can be covered with separate emphasis. It is therefore estimated that a larger number of mirrors will provide more improvement. However, more mirrors also imply a greater physical cost and complexity of the mirror array and its drivers.

With measurements or assumptions of the blur and achievable tilt angle of an AMA mirror, the allocation system can be used to simulate the projector's effectiveness. Test images were chosen to give different views into the behavior of the system. Figure 7a has a dark section at the bottom and a section of high intensity in the sky and on the peak of the mountain. The second test image, in Figure 7b, also has a bright sky region, but most of the darker regions are interspersed with brighter regions, which will make it more difficult to move light from one region to another without affecting fine detail. The third (Figure 7c) is an artificial test pattern that is often used to evaluate the contrast of video projectors.

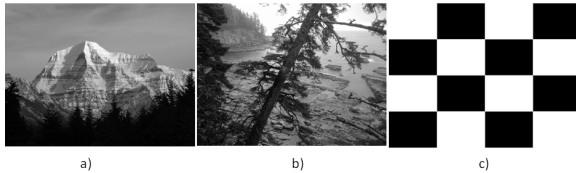


Figure 7: Test images: a) Mt. Robson, b) Rocky beach, c) ANSI Checkerboard.

Each test image and algorithm was simulated for a range of blur levels, number of mirrors, and light spot range. The median cut algorithm detailed above was compared against the Gaussian pyramid algorithm from [Hoskinson and Stoeber 2008]. For each condition, the improvement factor k was recorded. This gave a large matrix of

data that was used to qualitatively analyze the effect of each condition. A selection of results for 30mm disparity and 400 pixel range is given in Table 1.

	Array	G. pyramid		Median cut	
		100%	99.5%	100%	99.5%
Mt. Robson	3 × 3	2.48	3.05	1.65	3.55
	7 × 4	2.53	3.61	1.74	3.56
	10 × 10	2.30	3.16	1.80	3.57
Rocky beach	3 × 3	1.49	2.04	1.47	1.87
	7 × 4	1.72	1.88	1.77	1.95
	10 × 10	1.34	1.90	1.39	2.57
Checkerboard	3 × 3	1.01	1.01	1.00	1.01
	7 × 4	1.15	1.17	1.00	1.14
	10 × 10	1.12	1.25	1.03	1.25

Table 1: Improvement factors for different configurations and test images (simulation results). Results are listed for the cases where 100% and 99.5% of pixels are sufficiently illuminated.

For all tested algorithms, limiting the mirror movement to below 200 pixels severely impacts the possible improvement factor, irrespective of blur level or mirror numbers. Since range depends on disparity and mirror tilt angle, smaller ranges are easier to engineer and result in less clipping. The more separately-controllable mirrors in the array, the better the opportunity for improvement, because they offer more degrees of freedom to tailor the light distribution on the DMD to the desired image. The selection of results in Table 1 (values for 100%) shows that significant improvements are possible for a range of physically feasible parameters.

5.1 Allowing under-illuminated pixels

The results show that the choice of algorithm has a large impact on the improvement factor. This could be due to the algorithms' sensitivity to outliers. The improvement factor is set by the pixel with the minimum ratio of light given to light required (I_p/I_m). All it takes is one outlying pixel to bring down the improvement factor. If a particular pixel is an outlier, it may be that the rest of the image could have been shown at a much higher brightness if that pixel were ignored, with little perceivable loss. We tested how much brighter the image could get if we allowed a certain percentage of pixels to be under-illuminated compared to the rest of the image.

Figure 8 shows the performance of the three algorithms tested for the Mt. Robson image, with a blur from 60 mm disparity, an AMA with 7×4 mirrors, and a range of 300 pixels. For the case in which all pixels receive enough light, the pyramid (GP) representation scores highest with a 2.44 improvement factor, while median cut with iterative adjustment (MCIA) scores 2.32, and just using MC placement scores 1.9.

But at just 20 under-illuminated pixels (which, for an 800x600 image, is 0.004%), GP is overtaken by both median cut versions. GP scores 2.71, while MC alone scores 2.8, and MCIA scores 3.07. That is a 26% increase in brightness over the highest score obtained for perfect reconstruction. The increase raises to 36% if 50 pixels are allowed to be under-illuminated. The other two images tested are consistent with this trend. Figure 8 shows that the median cut algorithms are sensitive to outliers, and much more overall brightness increases can be achieved if the requirements are loosened.

Even if allowing under-illuminated pixels is not desirable under normal conditions, these tests show that there is a lot of flexibility to tailor the performance to different conditions. For instance, when displaying a video sequence on an AMA projector, the potential improvement factor will vary over time as the image changes,

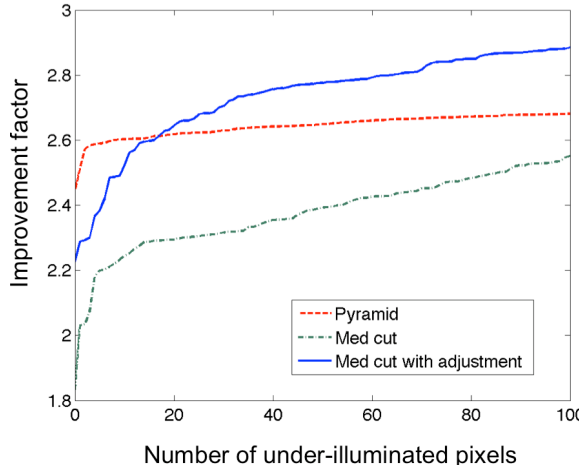


Figure 8: Improvement factor increase for the Mt. Robson image in Figure 7 when allowing some of the $600 \times 800 = 480000$ total pixels to be under-illuminated.

depending on the sum total intensity in the image and its distribution. If it changes too quickly or the magnitude of the change is too abrupt, the viewer will notice the artificial change in relative brightnesses of the different features in the image. Figure 8 shows that fixing the improvement factor for this video sequence doesn't necessarily mean fixing it at the minimum value out of all images in the sequence. By allowing some pixels to be under-illuminated, the improvement factor can be set at a higher level that matches what is achievable for an average image in the sequence, not the minimum.

5.2 Estimated system performance

Adding the AMA will incur some light losses that partially offset the gains described above. We can estimate the efficiency of a production version of the AMA at reflecting incident light by comparing it to the DMD. The DMD reflects $e_D = 68\%$ of incident light [Texas Instruments 2005]. The fill-factor of the AMA could be increased, because the AMA requires fewer mirrors than the DMD, and thus could have less total space between them. Also, the AMA will replace an existing fold mirror in the projector, which cancels out reflectance losses. Assuming an average tilt angle of 2.5° , the expected loss from clipping is 10% from Figure 4. Given these assumptions, we estimate the efficiency of the AMA as $e_A = 74\%$. Although this represents a significant loss of light, we still anticipate that the AMA-enabled projector would have a net gain of peak brightness. With 40mm blur disparity and 300 pixel range, the average improvement factor was 1.61, giving a net improvement factor of 1.20 after taking into account these losses. If we allow some pixels to remain under-illuminated, the case becomes even stronger. With 200 under-illuminated pixels, the average score for the median cut algorithm with iterative adjustment was 3.07. After taking into account losses, this still leaves a factor of 2.25 improvement.

5.3 Image fidelity

The addition of an AMA potentially introduces image distortions that can be attributed to the following main sources:

Quantization. There are only 256 greyscale values in a DLP. There will thus be errors due to quantization as the DMD cannot compensate accurately enough for the continuous, non-homogeneous illumination from the AMA.

Over-illumination. Over-illumination occurs because of light leakage due to the limited contrast of light modulators, and becomes non-uniform as the backlight is modulated. To estimate the amount of leakage in a projector for a given amount of luminance, the native contrast ratio of the device and peak brightness is measured. If the peak brightness of the projector is x , and contrast ratio is $1 : y$, then the estimated brightness of a pixel set to its darkest level in the DMD is x/y . If the pixel is set to a brightness of z , the estimated result is $z + x/y$. While this is not a perfect estimate due to the variability of lens scattering and possible non-linear effects, it provides a base level to compare the difference in an AMA-projector to a conventional projector.

Under-illumination. As mentioned above, it is possible to sacrifice some accuracy for overall brightness by allowing some pixels to be under-illuminated compared to the rest of the image. We can ensure this does not happen by specifying to the allocation algorithm that all pixels must have sufficient light, but how many under-illuminated pixels could be present without adversely affecting the viewing experience, and under what conditions?

To quantify the effect of these inaccuracies, the simulated optical combination of the AMA image on the DMD (I_P) and the DMD image are compared against the original image using an automated visual difference predictor designed for high dynamic range images as well as conventional images [Mantiuk et al. 2005]. The VDP algorithm provides a metric to distinguish the subset of differences between two images that a standard human observer would be able to detect. Our objective is to establish visual equivalence between images made with an AMA-equipped projector, compared to a regular projector that has the same peak brightness as the *improved* image.

We tested the configuration of a 7×4 array of mirrors with a range of 300 pixels, and a PSF with a full-width at half-maximum of 297 pixels. With DMD pixels being approximately $14\mu\text{m}$ square, the micromirror mechanical tilt angle needed to traverse 300 pixels is $\pm 2^\circ$, which is well within the range of published micromirrors [Hoskinson et al. 2010; Tsai et al. 2008]. I_p is a continuously-varying analog distribution on the DMD, and thus simulating quantization can be done by only quantizing I_{DMD} . The limited contrast of the projector is simulated by adding a portion of I_p to the resulting image.

$$I_{mc} = I_{DMD} + I_p/c, \quad (7)$$

where c refers to the contrast ratio of the DMD. For instance, if we take a conservative value of $1 : 400$ contrast ratio for the DMD, c is 400. I_{mc} is compared against kI_m , where k is the improvement factor.

With quantization taken into account, the VDP algorithm predicted that there was a probability of detection $P > 95\%$ for 0.0002% of the pixels, as shown in Figure 9a. For an 800×600 image, this works out to 96 pixels. The affected pixels are hardly visible at the bottom right-hand corner of the image.

Given that quantization and contrast issues did not significantly affect the image at this peak brightness, there is potential to significantly increase the overall brightness of the image if the constraints for perfect reproduction are relaxed. Table 2 shows the results of increasing the improvement factor to various levels, depending on the percentage of pixels that become under-illuminated. For 0.01% pixel error, which would allow for an improvement factor of 2.77, VDP calculated that only 0.0002% of pixels might be noticed. That is the same as the VDP result when all pixels are sufficiently illuminated, and only contrast and quantization artifacts are taken into



Figure 9: VDP results from testing the effect of quantization, limited contrast and a) allowing no under-illuminated pixels, b) allowing 2% under-illuminated pixels

account. I_p is not modified with these tests, just the image sent to the DMD. Also, it is not necessarily the brightest pixels that are under-illuminated; they could be anywhere in the image. In this particular image they start out in the bottom corner from where light has been redirected to other brighter parts of the image.

Percentage pixels under-illuminated	improvement	fraction of pixels $P > 95\%$
0.0	2.22	0.0002%
0.01	2.77	0.0002%
0.1	3.32	0.0065%
1.0	3.89	0.0923%
2.0	4.29	0.37%
5.0	5.07	1.13%

Table 2: Results of allowing a percentage of pixels to be under-illuminated.

The results in Table 2 show that there is a significant potential for further increase of peak brightness if the constraints for perfect results are relaxed. More than 5× improvement can be obtained with 5% of pixels under-illuminated. The VDP statistics suggest it is possible to obtain a substantially better improvement without sacrificing visual quality. When the peak brightness is inflated too much, however, artifacts become easily recognizable. Subjectively, there was a big jump between 1% and 2% of pixels underexposed; the extra 1% seems to come mostly from the central peak highlight, as shown in Figure 9b.

6 Physical realization

Analog micromirror arrays are at this stage still experimental platforms that are available only as prototypes from MEMS research labs. As such, existing chips still suffer from reliability issues, as well as permanent faults such as stuck mirrors, making it difficult to develop fully functioning prototypes of our projector design.

For our physical implementation, we therefore employ a custom, 7×4 AMA device, whose design we describe elsewhere [Hoskinson et al. 2010]. Due to fabrication problems, our prototype AMA chip had only 20 out of the 28 mirrors functional along both tilt axes. Using this chip we were able to build a first proof-of-concept prototype projector utilizing our optical design. The components of our system are mounted on an optical table to allow for precise adjustments. The projector is currently a black&white device, but color could be added with a filter wheel. In the future, using a filter wheel could allow for differential illumination of each color, which may provide additional advantages. The left image in Figure 1 shows a photo of the system with labels for the individual components.

6.1 Optical system

Adding the AMA to an existing projector without modifying any of the other optical components proved impractical due to the small size of the cavity that encloses the end of the integrating rod, folding mirror and the DMD, where the AMA would have had to be placed. The cavity was too small to place the AMA and still have adequate room for a relay lens between the AMA and DMD.

Instead, one projector was used as a light source, cutting a hole to allow the light from the lamp to exit the projector before it reaches its DMD. The light is collected with a 60mm lens and directed to the AMA. A 45mm lens relays the light from the AMA to a second projector, a Mitsubishi PK20 projector that is relatively easy to open up to allow access to the DMD. The light incident on the DMD is reflected normally through a prism to the PK20 projection lens onto a screen. Figure 1 shows a photograph of the prototype.

A signal splitter is used to send the same VGA signal to both projectors, so there is frame-level synchronization. Since the VGA signal does not dictate the orders of colors in a color-sequential display, the colors within the frame are not synchronized, and so are not correct. For this reason, we use only greyscale images with the prototype.

6.2 AMA driver

As shown in Figure 10, the micromirror array is electrically connected to a small printed circuit board though a socket that allows for easy chip insertion and removal. A VGA signal to the DMD is synchronized with 20 nanosecond accuracy to the AMA mirror control. This level of synchronization provides the opportunity for sub-video-frame synchronization between the AMA and the DMD, so that AMA mirrors could move to multiple positions within one frame of video.

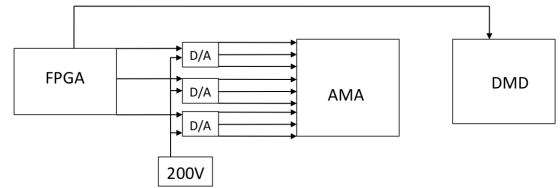


Figure 10: Schematic of the control signal flow in the prototype.

Due to problems with the micromirror fabrication, no fully-functional AMA chips were available for integration into the prototype. The goal was therefore to validate the main claims of the work by showing that regions of the image can be made brighter or darker, while still keeping the DMD image undistorted. Net gains in brightness compared to an unmodified projector were not pursued because a different light source was used, and the light path was significantly changed, resulting in some light losses.

6.3 Results

Figures 11 and 12 show the effect of different placements for the AMA device according to Section 3.1. Figure 11 illustrates the effect of changing the disparity on the level of blur. As the blur increases, details of the AMA disappear, and the resulting light spot becomes more and more disperse even as the displacement of the light spot increases. Note that these images can only provide qualitative comparisons of the blur amounts, but not of the relative dis-

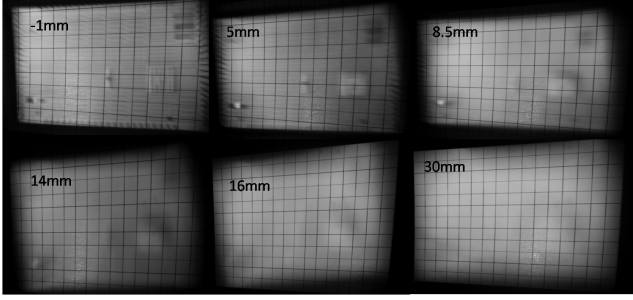


Figure 11: Images showing the output of the AMA prototype with different separation settings. The DMD is showing a black grid of 50 pixels squares on a white background. One AMA mirror in the center right of each image has been actuated.

placement, since changes in the alignment of the components make it impossible to make positional comparisons.

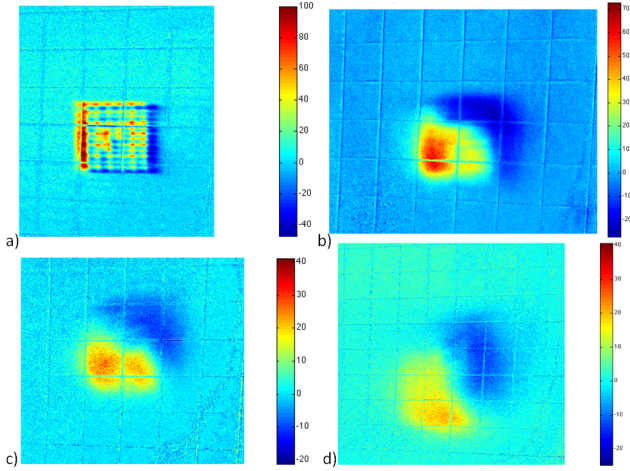


Figure 12: light spot at different disparities, units of percent difference. a)-1mm b) 8.5mm, c)14mm d) 30mm

In Figure 12, we examine the region affected by the tilted mirror from Figure 11. The mirror is tilted at 2.25° . To more clearly show the areas of relative change that we are concerned about, the intensity of these images is shown in units of percentage difference, calculated as

$$P_d = 100 \frac{I_t - I_n}{I_n}, \quad (8)$$

where I_t is the image with actuated AMA mirrors, I_n is the image of non-actuated mirrors, and P_d the resulting percentage difference.

Figure 12a shows the light spot nearly in focus, with a slight bias in light to the top left. At such low disparities, the light spot hardly moves at all. The mirror is tilting the light towards the top left, showing that the separation is actually slightly negative. If the DMD had been exactly on the focal plane, the light spot would not have been displaced at all, except from the bending artifacts that occur when these mirrors are actuated. The size of the light spot is approximately 75 pixels along each side.

Figure 12b shows how the light spot has become blurred as the disparity increases to 8.5mm. The size of the light spot has grown to

100 pixels per side, and has started to change shape due to mirror bending. The light spot has been displaced 60 pixels in a diagonal direction towards the bottom left. The actual light spot is less wide than the region it is leaving because of bending artifacts in the mirror. At 14mm disparity, the size of the light spot is now 120 pixels on its longest side, as shown in Figure 12c. The light spot has been displaced approximately 90 pixels. Figure 12d shows the light spot at 30mm of disparity. Although hardly visible in Figure 11, showing a closeup of the region in false color reveals that the light spot has shifted 160 pixels. The light spot is further elongated, and now is spread over an area of 160 pixels per side. Also evident is that the peak intensity change attenuates with the blur. At very low levels of blur such as 8.5mm, there is a 75% improvement in peak brightness, and a 25% decrease in peak darkness. At 30mm of disparity, the peak has been reduced to a 40% increase, and 25% decrease. The non-symmetrical nature of these increases are likely caused by bending artifacts of the AMA mirrors, as the light spot becomes clearly smaller than the space it leaves as the disparity increases.



Figure 13: Projection of a natural image. Left: the source image. Center: the allocation of light from the light spot image. Right: photograph of the projected image (different exposures are shown in Figure 1).

Figures 13 and 1 show a result for an natural image projected on our prototype, using a disparity of 15 mm. Even with some defective mirrors and mirrors that can only move along one dimension, the light spot image has a contrast of about 2.6:1. This ratio represents the improvement in contrast over a uniform source of illumination, and gets multiplied with the DMD contrast for the final contrast of the projected image.

Overall, our results show that the approach of using an AMA is successful at redistributing light from one region of the projected image to another. We also demonstrated that the AMA does not geometrically distort the image from the DMD in any way. The effect that disparity has on both range and blur was shown, and validates the approach to simulations taken in Section 4.

7 Conclusions

We have presented a method to significantly improve the brightness and contrast capability of a projector through the addition of an analog micromirror array. By reallocating light to where it is needed, and removing it from where it is not, an AMA projector makes better use of its light source, which is one of the most expensive components of today's projectors. After the addition of an AMA, the light reaching the primary image modulator, such as a DMD, is no longer uniform. The light distribution from the AMA mirrors is simulated, and the compensation for the non-homogeneity is applied to the original image before it is sent to the DMD. The result is an image of higher contrast and peak brightness with the same projection lamp.

We have demonstrated that an AMA-enhanced projector can make projectors intelligent allocators of their light sources. While our current proof-of-concept implementation suffers from the experimental nature of available AMA devices, we believe that implementations with serially produced AMA devices will significantly

improve contrast in future commercial projector systems, while allowing for less expensive lamps, lower heat production, and smaller projector form factors.

Acknowledgments

We would like to acknowledge the fabrication provided by CMC Microsystems (www.cmc.ca) that facilitated this research. This work was in part supported by Dolby Labs, the Institute for Mathematics of Information Technology and Complex Systems (MITACS), and the National Science and Engineering Research Council (NSERC).

References

- AGARWAL, P., AND VARADARAJAN, K. 2004. A near-linear constant-factor approximation for euclidean bipartite matching? In *Proceedings of the twentieth annual symposium on Computational geometry*, ACM New York, NY, USA, 247–252.
- BIMBER, O., AND IWAI, D. 2008. Superimposing dynamic range. *ACM Trans. Graph. (Proc. Siggraph Asia)* 27, 5, 1–8.
- BLOOM, D., 1997. The grating light valve: revolutionizing display technology.
- BRENNESHOLTZ, M. S., AND STUPP, E. H. 2008. *Projection Displays*, 2nd ed. Wiley.
- DAMBERG, G., SEETZEN, H., WARD, G., HEIDRICH, W., AND WHITEHEAD, L. 2007. High Dynamic Range Projection Systems. *Proceedings of the 2006 Society for Information Display Annual Symposium*.
- DEBEVEC, P. 2005. A median cut algorithm for light probe sampling. In *SIGGRAPH '05: ACM SIGGRAPH 2005 Posters*, ACM, New York, NY, USA, 66.
- DERRA, G., MOENCH, H., FISCHER, E., GIESE, H., HECHTFISCHER, U., HEUSLER, G., KOERBER, A., NIEMANN, U., NOERTEMANN, F., PEKARSKI, P., ET AL. 2005. UHP lamp systems for projection applications. *JOURNAL OF PHYSICS-LONDON-D APPLIED PHYSICS* 38, 17, 2995.
- DEWALD, D., SEGLER, D., AND PENN, S. 2004. Advances in contrast enhancement for DLP projection displays. *Journal of the Society for Information Display* 11, 177–181.
- HALBACH, K. 1964. Matrix representation of Gaussian optics. *American Journal of Physics* 32, 90.
- HECHT, E. 2002. *Optics*, 4th ed. Addison Wesley, San Francisco, CA, USA.
- HECKBERT, P. 1982. Color image quantization for frame buffer display. *ACM SIGGRAPH Computer Graphics* 16, 3, 297–307.
- HOSKINSON, R., AND STOEBER, B. 2008. High-dynamic range image projection using an auxiliary mems mirror array. *Optics Express* 16, 7361–7368.
- HOSKINSON, R., BUESCHER, D., HAMPL, S., HOLLE, M., AND STOEBER, B. 2010. Arrays of large-area, large-angle tip/tilt micromirrors for use in a high-contrast projector. In submission.
- IISAKA, H., TOYOOKA, T., YOSHIDA, S., AND NAGATA, M. 2003. Novel Projection System Based on an Adaptive Dynamic Range Control Concept. In *Procoeedings Int Disp Workshops*, vol. 10, 1553–1556.
- KUHN, H. 1955. The Hungarian method for the assignment and transportation problems. *Naval Research Logistics Quarterly* 2, 83–97.
- KUSAKABE, Y., KANAZAWA, M., NOJIRI, Y., FURUYA, M., AND YOSHIMURA, M. 2009. A high-dynamic-range and high-resolution projector with dual modulation. In *Proceedings of SPIE*, vol. 7241.
- MANTIUK, R., DALY, S., MYSZKOWSKI, K., AND SEIDEL, H.-P. 2005. Predicting visible differences in high dynamic range images - model and its calibration. In *Human Vision and Electronic Imaging X, IS&T/SPIE's 17th Annual Symposium on Electronic Imaging* (2005), B. E. Rogowitz, T. N. Pappas, and S. J. Daly, Eds., vol. 5666, 204–214.
- NAGAHARA, H., KUTHIRUMMAL, S., ZHOU, C., AND NAYAR, S. 2008. Flexible Depth of Field Photography. In *European Conference on Computer Vision (ECCV)*.
- PAVLOVYCH, A., AND STUERZLINGER, W. 2005. A High-Dynamic Range Projection System. *Progress in biomedical optics and imaging* 6, 39.
- SEETZEN, H., HEIDRICH, W., STUERZLINGER, W., WARD, G., WHITEHEAD, L., TRENTACOSTE, M., GHOSH, A., AND VOROZCOVS, A. 2004. High dynamic range display systems. *ACM Transactions on Graphics (Siggraph 2004)* 23, 3, 760–768.
- SEETZEN, H. 2009. *High Dynamic Range Display and Projection Systems*. PhD thesis, University of British Columbia.
- TEXAS INSTRUMENTS. 2005. *DMD 0.7 XGA 12 DDR DMD Discovery*.
- TOYOOKA, T., YOSHIDA, S., AND IISAKA, H. 2005. Illumination control system for adaptive dynamic range control. *Journal of the Society for Information Display* 13, 105.
- TSAI, J., CHIOU, S., HSIEH, T., SUN, C., HAH, D., AND WU, M. 2008. Two-axis MEMS scanners with radial vertical combdrive actuators—design, theoretical analysis, and fabrication. *Journal of Optics A: Pure and Applied Optics* 10, 044006.